11 May 2024

ALMA MATER STUDIORUM
UNIVERSITÀ DI BOLOGNA

ARCHIVIO ISTITUZIONALE
DELLA RICERCA

Alma Mater Studiorum Università di Bologna
Archivio istituzionale della ricerca

Anisotropy and the Onset of the Thermoconvective Instability in a Vertical Porous Layer

This is the final peer-reviewed author's accepted manuscript (postprint) of the following publication:

Published Version:
Anisotropy and the Onset of the Thermoconvective Instability in a Vertical Porous Layer / Barletta, A.; Celli, M.. - In: JOURNAL OF HEAT TRANSFER. - ISSN 0022-1481. - STAMPA. - 143:10(2021), pp. 102601.1-102601.5. [10.1115/1.4051322]

This version is available at: https://hdl.handle.net/11585/832527 since: 2023-01-11

Published:

DOI: http://doi.org/10.1115/1.4051322

Terms of use:

Some rights reserved. The terms and conditions for the reuse of this version of the manuscript are specified in the publishing policy. For all terms of use and more information see the publisher's website.

(Article begins on next page)

This item was downloaded from IRIS Università di Bologna (https://cris.unibo.it/).
When citing, please refer to the published version.

This is the final peer-reviewed accepted manuscript of:

Barletta, A. and Celli, M

Anisotropy and the Onset of the Thermoconvective Instability in a Vertical Porous Layer

In:

ASME. Journal of Heat Transfer. October 2021; 143(10)

The final published version is available at:

https://doi.org/10.1115/1.4051322

Rights / License:

The terms and conditions for the reuse of this version of the manuscript are specified in the publishing policy. For all terms of use and more information see the publisher's website.

Anisotropy and the Onset of the Thermoconvective Instability in a Vertical Porous Layer

A. Barletta, M. Celli

Department of Industrial Engineering
Alma Mater Studiorum Università di Bologna
Viale Risorgimento 2
40136, Bologna, Italy
Email: antonio.barletta@unibo.it
Email: michele.celli3@unibo.it

The thermoconvective instability of the parallel vertical flow in a fluid saturated porous layer bounded by parallel open boundaries is studied. The open boundaries are assumed to be kept at constant uniform pressure while their temperatures are uniform and different, thus forcing a horizontal temperature gradient across the layer. The anisotropic permeability of the porous layer is accounted for by assuming the principal axes to be oriented along the directions perpendicular and parallel to the layer boundaries. A linear stability analysis based on the Fourier normal modes of perturbation is carried out by testing the effect of the inclination of the normal mode wave vector to the vertical. The neutral stability curves and the critical Rayleigh number for the onset of the instability are evaluated by solving numerically the stability eigenvalue problem.

Nomenclature

$f(x), h(x)$ Eigenfunctions.
$\mathbf{g}$ Gravitational acceleration.
g Modulus of $\mathbf{g}$.
k Wave number.
k_y, k_z Wave vector components.
$\underline{\mathbf{K}}$ Permeability.
K_L, K_T Permeability components.
L Slab thickness.
P Difference between the pressure and the hydrostatic pressure.
Ra Rayleigh number.
S Scaled Rayleigh number, $S = k_z Ra/k$.
t Time.
T Temperature.
T_0 Reference temperature, $T_0 = (T_1 + T_2)/2$.
T_1, T_2 Boundary temperatures.
$\mathbf{u}$ Seepage velocity, $\mathbf{u} = (u, v, w)$.
x, y, z Cartesian coordinates.

Greek Symbols

α Average thermal diffusivity.
β Coefficient of thermal expansion for the fluid.
λ Complex growth rate.
μ Dynamic viscosity.
ξ Anisotropy parameter.
ρ_0 Reference fluid density.
σ Heat capacity ratio.

Superscripts, Subscripts

$*$ Dimensionless quantities in equation (5).
$\sim$ Perturbations.
v Scaled quantities in equations (15) and (17).
b Basic solution.
c Critical values.
t Tip values.

1 Introduction

The emergence of the thermoconvective instability in a fluid system is a typical feature of a horizontal fluid layer or fluid saturated porous layer where conduction heat transfer changes into convection due to a vertical downward temperature gradient. This phenomenon is typical of the Rayleigh–Bénard system, where a horizontal fluid layer is bounded by isothermal planes kept at different temperatures yielding conditions of heating from below [1]. As is well–known, a version of the Rayleigh–Bénard stability problem involving a layer of fluid saturated porous medium has been studied in the classical papers by Horton and Rogers [2] and by Lapwood [3]. Nowadays, the porous medium version of the Rayleigh–Bénard problem is either known as Darcy–Bénard problem or Horton–Rogers–Lapwood problem [4–6].

The onset of multicellular convection patterns is a typical phenomenon also for vertical fluid layers [7–9], where a side–heating configuration is induced by boundaries kept at

different uniform temperatures. Interestingly enough, the onset of multicellular convection patterns destabilizing the conduction regime was ruled out in the case of a vertical porous slab. This conclusion is a consequence of a pioneering paper by Gill [10]. In fact, Gill proposed a rigorous proof of the absence of thermoconvective instability in a vertical porous slab saturated by a fluid and bounded by isothermal and impermeable sidewalls. Other authors further enhanced Gill's results by taking into account other effects or developing a nonlinear stability analysis [11–15]. Only recently, evidence that thermoconvective instability can indeed arise in a vertical porous layer has been given [16]. The key argument is the observation that Gill's proof of stability relies on the assumption that the boundaries are impermeable. When this assumption is relaxed, then the thermoconvective instability is possible at sufficiently large Rayleigh numbers.

Most of the studies regarding the onset of the thermoconvective instability in a fluid saturated porous medium are based on the model of isotropic permeability. The permeability is considered as a scalar, while for anisotropic porous materials it is modelled as a second–rank tensor. Anisotropy effects may be significant in several materials of engineering interest. Thus, some authors extended the knowledge on the thermoconvective instability in porous media by envisaging anisotropic materials [5, 17, 18]. Among these papers, we mention the studies by Kvernvold and Tyvand [19] and by Nilsen and Storesletten [20], where the Rayleigh–Bénard instability is reconsidered for an anisotropic porous medium, as well as the analysis carried out by Rees and Postelnicu [21], where the effect of the porous layer inclination to the horizontal is taken into account. Very recent developments on the onset of the thermoconvective instability in anisotropic porous media have been achieved by Straughan [22], by Storesletten and Rees [23] and by Naveen *et al.* [24]. The latter contribution is of special interest for the present paper as it provides an extension of Gill's analysis [10] to the case of an anisotropic porous medium.

The aim of this paper is to provide an extension of the study carried out by Barletta [16] by envisaging a situation where the porous material has an anisotropic permeability. More precisely, we will consider a vertical porous slab with open boundaries, modelled as isobaric planes, kept at unequal uniform temperatures. The permeability is considered as anisotropic, meaning that it is given by a second–rank tensor. The principal axes will be assumed to be transversal and longitudinal with respect to the plane slab, thus following the description adopted by Storesletten and Rees [23]. The stability of the basic parallel buoyant flow in the slab will be studied by adopting a modal analysis. The stability eigenvalue problem will be solved numerically by employing the shooting method. The effects of the anisotropy will be discussed for the neutral stability curves and for the critical values of the wave number and of the Rayleigh number.

2 Mathematical Model

We consider a vertical porous slab and a Cartesian coordinate system with the x axis horizontal and perpendicular to the slab, the y axis horizontal and parallel to the slab, and the z axis vertical and parallel to the slab. The origin of the axes is in the slab vertical midplane. The slab is assumed to be infinitely wide in the y and z direction, while its thickness is L. A sketch of the slab cross–section in the xz plane is given in Fig. 1. The permeable side boundaries at $x = \pm L/2$ are kept at a uniform hydrostatic pressure and uniform temperatures T_1 and T_2, with $T_2 > T_1$.

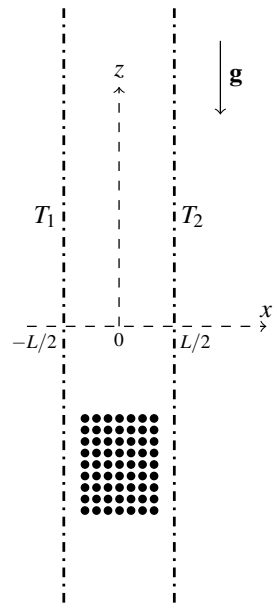

Fig. 1. A sketch of the vertical porous slab

2.1 Governing Equations

The fluid saturated porous medium is anisotropic with principal axes directed along the (x, y, z) axes. The local momentum balance equation is modelled according to Darcy's law including the buoyancy force, namely [5]

$$\mu \mathbf{u} = -\underline{\mathbf{K}} \left[\nabla P + \rho_0 \beta \left(T - T_0 \right) \mathbf{g} \right], \tag{1}$$

where the permeability tensor is expressed as

$$\underline{\mathbf{K}} = \begin{pmatrix} K_T & 0 & 0 \\ 0 & K_L & 0 \\ 0 & 0 & K_L \end{pmatrix}. \tag{2}$$

Equation (2) is a special case of anisotropic permeability where one direction, the transverse x axis, is selected out of the other two longitudinal y and z directions. This is typical of fibrous or layered porous media where the direction of the fibres or layers displays an hydraulic resistance different from that of the other directions [17, 23].

According to the Oberbeck–Boussinesq approximation, the only effect of the temperature–dependent density is the buoyancy force so that the mass, momentum and energy bal-

ance equations can be written as [5, 23]

$$\frac{\partial u}{\partial x}+\frac{\partial v}{\partial y}+\frac{\partial w}{\partial z}=0, \tag{3a}$$

$$u=-\frac{K_T}{\mu}\frac{\partial P}{\partial x}, \tag{3b}$$

$$v=-\frac{K_L}{\mu}\frac{\partial P}{\partial y}, \tag{3c}$$

$$w=-\frac{K_L}{\mu}\left[\frac{\partial P}{\partial z}-\rho_0\beta g\,(T-T_0)\right], \tag{3d}$$

$$\sigma\frac{\partial T}{\partial t}+u\frac{\partial T}{\partial x}+v\frac{\partial T}{\partial y}+w\frac{\partial T}{\partial z}=\alpha\nabla^2 T. \tag{3e}$$

Here, σ is the ratio between the heat capacity of the saturated porous medium and that of the fluid. Following Barletta [16], the boundary conditions can be written as

$$\begin{aligned} &P=0, \quad T=T_1 \quad \text{in} \quad x=-L/2,\\ &P=0, \quad T=T_2 \quad \text{in} \quad x=L/2. \end{aligned} \tag{4}$$

In order to keep the complexity of the anisotropy model at its minimum, we assumed an isotropic thermal diffusivity, while the most general situation would imply, at the right hand side of equation (3e), a term

$$\nabla\cdot(\underline{\alpha}\nabla T)$$

instead. Here, $\underline{\alpha}$ stands for the second–rank diffusivity tensor accounting for the thermal anisotropy. Since the thermal diffusivity α in equation (3e) comes out from a volume averaging of the conductivities of the solid and the fluid, we consider this parameter as one including average over the transverse and longitudinal directions as well. This simplification, similar to that adopted by Storesletten and Rees [23], will reduce the number of dimensionless parameters governing the onset of the instability.

2.2 Dimensionless Quantities

A nondimensional formulation of equations (3) is achieved by defining

$$\begin{aligned} (x^*,y^*,z^*)&=(x,y,z)/L, \quad t^*=t\,\alpha/(\sigma L^2),\\ (u^*,v^*,w^*)&=(u,v,w)\,L/\alpha, \quad P^*=P\,K_L/(\mu\alpha),\\ T^*&=(T-T_0)/(T_2-T_1), \end{aligned} \tag{5}$$

where the asterisks denote the dimensionless quantities. Hereafter, such asterisks will be omitted for the sake of brevity, as we will only deal with dimensionless quantities. Thus, the nondimensional reformulation of equations (3) and (4), based on the fields T and P, is given by

$$\xi\frac{\partial^2 P}{\partial x^2}+\frac{\partial^2 P}{\partial y^2}+\frac{\partial^2 P}{\partial z^2}=Ra\frac{\partial T}{\partial z}, \tag{6a}$$

$$\begin{aligned} \frac{\partial T}{\partial t}-\xi\frac{\partial P}{\partial x}\frac{\partial T}{\partial x}-\frac{\partial P}{\partial y}\frac{\partial T}{\partial y}-\left(\frac{\partial P}{\partial z}-Ra\,T\right)\frac{\partial T}{\partial z}\\ =\frac{\partial^2 T}{\partial x^2}+\frac{\partial^2 T}{\partial y^2}+\frac{\partial^2 T}{\partial z^2}, \end{aligned} \tag{6b}$$

and

$$P=0, \quad T=\pm 1/2 \quad \text{in} \quad x=\pm 1/2. \tag{7}$$

In equations (6), the anisotropy parameter ξ and the porous medium version of the Rayleigh number Ra are defined as

$$\xi=K_T/K_L, \quad Ra=[\rho_0\, g\,\beta\,(T_2-T_1)\,K_L\,L]/(\mu\alpha). \tag{8}$$

3 The Basic Flow

A basic flow solution driven by the buoyancy force is obtained in a stationary regime and with a purely vertical velocity field, namely

$$P_b=0, \quad T_b=x, \quad w_b=Ra\,x. \tag{9}$$

The basic flow rate is zero. In fact, the integral of w_b over the interval $-1/2\le x\le 1/2$ is zero.

4 Stability Analysis

Perturbations of the basic solution can be defined as

$$P=P_b+\tilde{P}, \quad T=T_b+\tilde{T}. \tag{10}$$

We substitute equation (10) into equations (6) and (7), we take into account equation (9) and we linearise the resulting equations by assuming that the strength of the perturbation is much smaller than that of the basic state. Thus, we obtain

$$\xi\frac{\partial^2\tilde{P}}{\partial x^2}+\frac{\partial^2\tilde{P}}{\partial y^2}+\frac{\partial^2\tilde{P}}{\partial z^2}=Ra\frac{\partial\tilde{T}}{\partial z}, \tag{11a}$$

$$\frac{\partial\tilde{T}}{\partial t}-\xi\frac{\partial\tilde{P}}{\partial x}+Ra\,x\frac{\partial\tilde{T}}{\partial z}=\frac{\partial^2\tilde{T}}{\partial x^2}+\frac{\partial^2\tilde{T}}{\partial y^2}+\frac{\partial^2\tilde{T}}{\partial z^2}, \tag{11b}$$

with boundary conditions

$$\tilde{P}=0, \quad \tilde{T}=0 \quad \text{in} \quad x=\pm 1/2. \tag{12}$$

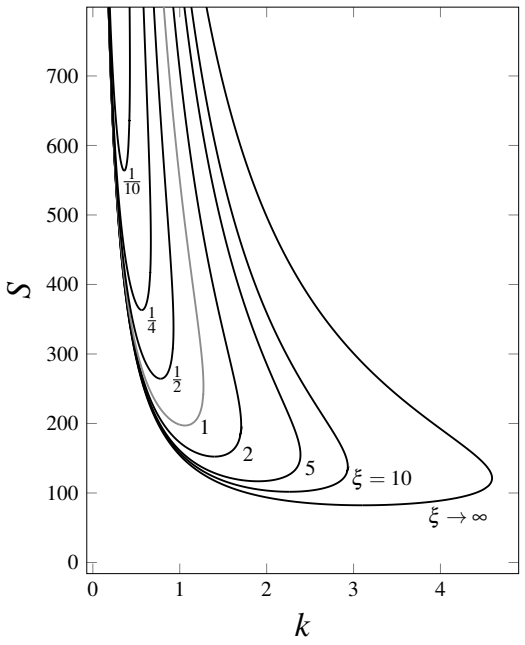

Fig. 2. Neutral stability curves in the (k,S) plane for different values of ξ

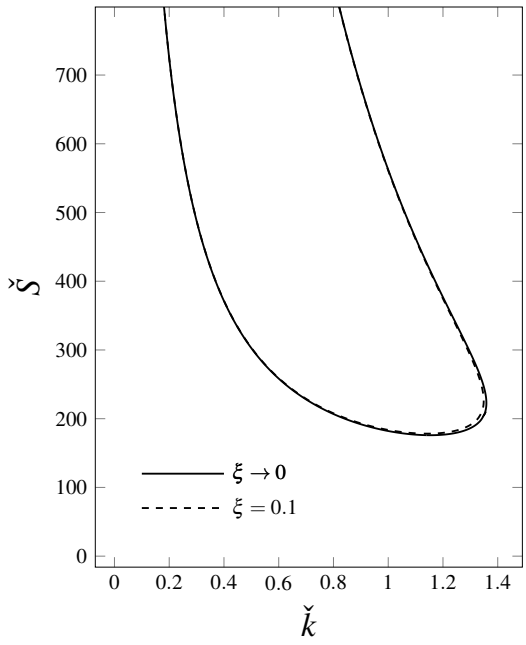

Fig. 3. Neutral stability curves in the $(\breve{k},\breve{S})$ plane for $\xi \to 0$

4.1 The Stability Eigenvalue Problem

We assume normal mode perturbations given by

$$\begin{bmatrix}\tilde{P}(x,y,z,t)\\ \tilde{T}(x,y,z,t)\end{bmatrix} = \begin{bmatrix}f(x)\\ h(x)\end{bmatrix} e^{i\left(k_y y + k_z z\right)} e^{\lambda t}. \tag{13}$$

Here, (k_y,k_z) are the components of the wave vector whose modulus, $k=(k_y^2+k_z^2)^{1/2}$, is the wave number. The growth rate of the perturbation is $\mathrm{Re}(\lambda)$, while $-\mathrm{Im}(\lambda)$ yields the angular frequency of the normal mode.

By substituting equation (13) in equations (11) and (12), we are lead to the stability eigenvalue problem,

$$\xi f'' - k^2 f - ikSh = 0, \tag{14a}$$
$$h'' - \left(\lambda + k^2 + ikSx\right)h + \xi f' = 0, \tag{14b}$$
$$f = 0, \quad h = 0 \quad \text{in} \quad x = \pm 1/2, \tag{14c}$$

where the primes denote derivatives with respect to x. In equations (14), we introduced the scaled Rayleigh number, $S = k_z Ra/k$.

A numerical solution of equations (14) yields the complex eigenvalue λ and the complex–valued eigenfunctions (f,h) for prescribed input values of (k,S,ξ). In this paper, the numerical technique adopted to achieve this task is the shooting method. Here, such method is exploited and coded along the lines described in chapter 10 of the book by Barletta [6]. The main purpose is determining the neutral stability condition where $\mathrm{Re}(\lambda)=0$. Such a condition marks the threshold of the transition from linear stability, $\mathrm{Re}(\lambda)<0$, to instability, $\mathrm{Re}(\lambda)>0$.

4.2 The Limiting Case $\xi \gg 1$

Let us introduce the scaled eigenfunction,

$$\breve{h} = \xi^{-1} h. \tag{15}$$

Then, by substituting equation (15) into equations (14), by simplifying wherever needed and by taking the limit $\xi \to \infty$, we get

$$f'' - ikS\breve{h} = 0, \tag{16a}$$
$$\breve{h}'' - \left(\lambda + k^2 + ikSx\right)\breve{h} + f' = 0, \tag{16b}$$
$$f = 0, \quad \breve{h} = 0 \quad \text{in} \quad x = \pm 1/2. \tag{16c}$$

Equations (16) are independent of ξ and, as such, they serve for capturing the neutral stability condition when ξ is infinitely large. Physically, this limit means a transverse permeability much larger than the longitudinal permeability, *i.e.* $K_T \gg K_L$.

4.3 The Limiting Case $\xi \ll 1$

We define the scaled parameter and eigenfunction,

$$\breve{k} = \xi^{-1/2} k, \quad \breve{S} = \xi^{1/2} S, \quad \breve{h} = \xi^{-1} h. \tag{17}$$

We substitute equation (17) into equations (14), simplify and take the limit $\xi \to 0$. Thus, we obtain

$$f'' - \breve{k}^2 f - i\breve{k}\breve{S}\breve{h} = 0, \tag{18a}$$
$$\breve{h}'' - \left(\lambda + i\breve{k}\breve{S}x\right)\breve{h} + f' = 0, \tag{18b}$$
$$f = 0, \quad \breve{h} = 0 \quad \text{in} \quad x = \pm 1/2. \tag{18c}$$

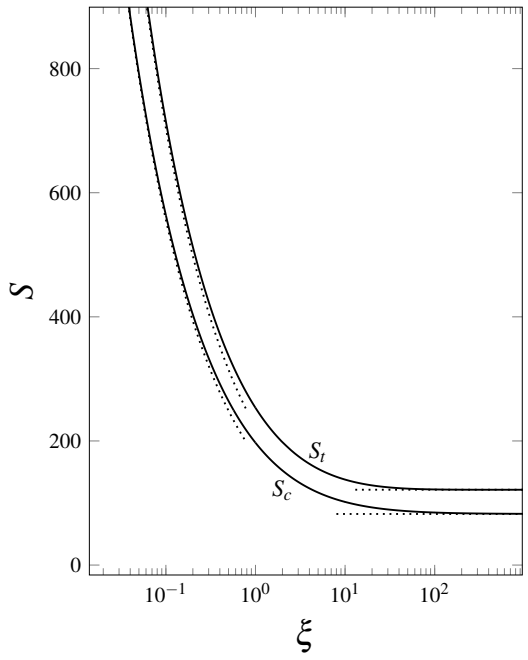

Fig. 4. Plots of the critical and tip values of S versus ξ. The dotted lines illustrate the asymptotic trends for small ξ and for large ξ

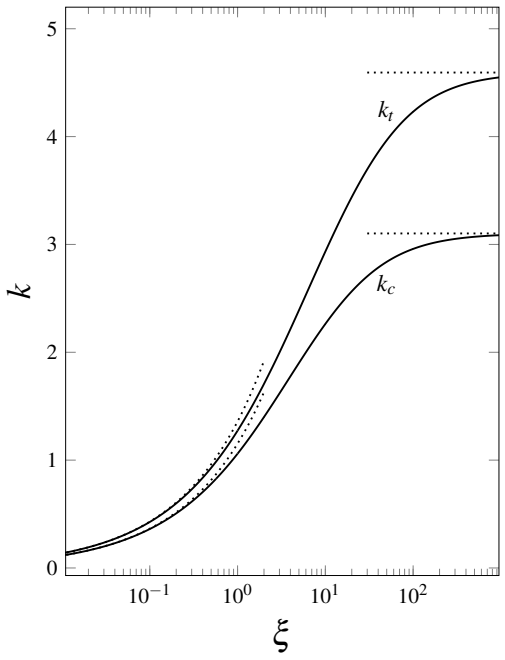

Fig. 5. Plots of the critical and tip values of k versus ξ. The dotted lines illustrate the asymptotic trends for small ξ and for large ξ

Once again, equations (18) define an eigenvalue problem independent of ξ which serves to describe the features of the neutral stability condition when $\xi \ll 1$, namely in an anisotropic medium where $K_L \gg K_T$.

5 Discussion of the Results

The first evident feature observed with the numerical solution of the eigenvalue problem (14) is that the eigenvalues are real or, equivalently, the angular frequency $-\mathrm{Im}(\lambda)$ is zero. This means that the onset of the thermoconvective instability reflects the principle of exchange of stabilities [1]. Such a behaviour has been already pointed out for the isotropic case [16]. We also note that the stability eigenvalue problem (14) coincides with that formulated by Barletta [16] in the isotropic case, $\xi = 1$ meaning $K_T = K_L$.

Figure 2 displays the neutral stability curves for different values of ξ. The isotropic case ($\xi = 1$) is evidenced with a grey line. The limiting case $\xi \to \infty$, obtained by solving equations (16) is also displayed. The instability arises within the region entrapped by the neutral stability curve. Hence, the minimum value of S along each neutral stability curve defines the critical values (k_c, S_c) which depend on ξ. Instability is possible for $S > S_c$. Thus, Fig. 2 shows clearly that the anisotropy is destabilising when $\xi > 1$, while it is stabilising when $\xi < 1$. This is physically sound as $\xi > 1$ means a larger hydraulic resistance for the longitudinal directions, y and z, than for the transverse x direction. This feature inevitably tends to favour the onset of cellular flow patterns over the basic vertical and, hence, longitudinal flow. Another feature typical of the teardrop–shaped neutral stability curves is that, for each ξ, there exists a maximum k position where $k = k_t$ and $S = S_t$. Here, the subscript t stands for "tip". With $k > k_t$, no instability is observed for a fixed ξ.

Table 1. Critical and tip values of k and S

ξ	k_c	S_c	k_t	S_t
0.1	0.3611961	563.6479	0.4265219	714.8381
0.5	0.7795100	264.3892	0.9281404	337.5210
1	1.059498	197.0812	1.272911	253.3400
1.5	1.252150	168.6391	1.516234	218.0511
2	1.399648	152.3492	1.706706	197.9887
5	1.900118	116.8669	2.389042	155.1100
10	2.262886	101.7467	2.933712	137.7329
100	2.958457	84.64271	4.230445	121.8534

Figure 3 explores the regime of small ξ, by comparing the neutral stability curves for $\xi \to 0$ and for $\xi = 1/10$ displayed in the $(\check{k}, \check{S})$ plane. We note that the two curves are almost overlapped suggesting that the regime $\xi \ll 1$ is almost attained when $\xi = 0.1$. We also point out that the numerical data for the limiting case $\xi \to 0$ have been obtained from the solution of the eigenvalue problem (18).

The critical and tip values of S are plotted versus ξ in Fig. 4. This figure illustrates also the asymptotic behaviour for both $\xi \gg 1$ and $\xi \ll 1$ obtained by solving equations (16) and equations (18), respectively. In particular, for the limiting case where $\xi \gg 1$, we have

$$k_c = 3.101992, \quad S_c = 82.32102,$$
$$k_t = 4.593909, \quad S_t = 121.3962. \tag{19}$$

On the other hand, for $\xi \ll 1$, we obtain

$$k_c = 1.153106\xi^{1/2}, \quad S_c = 175.9625/\xi^{1/2},$$
$$k_t = 1.358588\xi^{1/2}, \quad S_t = 222.7531/\xi^{1/2}. \qquad (20)$$

The asymptotic trends revealed by equation (20) show that the instability cannot arise when $\xi \to 0$ as the neutral stability curve is compressed to vanishingly small wave numbers and pushed to infinitely large values of S. This feature is also suggested by Fig. 2. Figure 5 is the dual part of Fig. 4 with the critical and tip values of the wave number k plotted versus ξ. Again, the dotted lines show the asymptotic solutions found in the limits $\xi \to \infty$ and $\xi \to 0$. Samples of the same sets of data are also reported in Table 1. We report that the numerical data for the isotropic case $\xi = 1$ perfectly coincide with those found in Barletta [16].

A final remark is for the role of the wave vector orientation for a given k, which means the interpretation of the data provided so far in terms of the Rayleigh number Ra, instead of its scaled counterpart S. By relying on its definition, $S = k_z Ra/k$, we immediately infer that the most unstable modes are those with $k_z = k$ or, equivalently, $k_y = 0$. Such two–dimensional modes are usually termed transverse rolls. That the instability arises with these modes is a feature that has been already pointed out, for the isotropic case, in Barletta [16].

6 Conclusions

The instability of the stationary and parallel flow in a vertical porous layer caused by the buoyancy force has been studied. The effect of the anisotropic permeability of the medium has been taken into account. The linear response to small–amplitude perturbations in the form of normal modes has been tested. The stability eigenvalue problem has been solved numerically for a wide range of the governing parameters, ξ (the anisotropy parameter) and Ra (the Rayleigh number).

The most important results of this analysis can be outlined as follows:

• The onset of the instability is due to the transverse rolls, namely the two–dimensional normal modes lying in the plane of the basic buoyant flow.

• When $\xi > 1$, which means a transverse permeability larger than the longitudinal permeability, the effect of the anisotropy is destabilizing. When $\xi < 1$, the longitudinal permeability is larger than the transverse permeability and the effect of anisotropy is stabilising.

• In the limit of very large values of ξ, the critical Rayleigh number attains the asymptotic value 82.32102, which is the lowest possible value for the onset of the instability in the anisotropic porous layer. In the limit of a vanishingly small ξ, no instability arises according to the linear analysis.

There are several possible future developments of the analysis reported in this paper. For instance, the nonlinear behaviour in the supercritical regime needs a specific study, focussed on the evaluation of the heat transfer rate across the porous layer and on the planforms of the multicellular patterns resulting from the instability.

Acknowledgements

The authors A. Barletta and M. Celli acknowledge the financial support from the grant PRIN 2017F7KZWS provided by the Italian Ministry of Education and Scientific Research.

References

[1] Drazin, P. G., and Reid, W. H., 2004. *Hydrodynamic Stability*. Cambridge University Press, Cambridge, UK.

[2] Horton, C. W., and Rogers, F. T., 1945. "Convection currents in a porous medium". *Journal of Applied Physics,* **16**, pp. 367–370.

[3] Lapwood, E. R., 1948. "Convection of a fluid in a porous medium". *Proceedings of the Cambridge Philosophical Society,* **44**, pp. 508–521.

[4] Straughan, B., 2008. *Stability and Wave Motion in Porous Media*. Springer, New York.

[5] Nield, D. A., and Bejan, A., 2017. *Convection in Porous Media*, 5th ed. Springer, New York.

[6] Barletta, A., 2019. *Routes to Absolute Instability in Porous Media*. Springer, New York.

[7] Vest, C. M., and Arpaci, V. S., 1969. "Stability of natural convection in a vertical slot". *Journal of Fluid Mechanics,* **36**, pp. 1–15.

[8] Shaaban, A. H., and Oẓisịk, M. N., 1983. "The effect of nonlinear density stratification on the stability of a vertical water layer in the conduction regime". *JOURNAL OF HEAT TRANSFER–TRANSACTIONS OF THE ASME,* **105**, pp. 130–137.

[9] Jin, Y. Y., and Chen, C. F., 1996. "Instability of convection and heat transfer of high Prandtl number fluids in a vertical slot". *JOURNAL OF HEAT TRANSFER–TRANSACTIONS OF THE ASME,* **118**, pp. 359–365.

[10] Gill, A. E., 1969. "A proof that convection in a porous vertical slab is stable". *Journal of Fluid Mechanics,* **35**, pp. 545–547.

[11] Rees, D. A. S., 1988. "The stability of Prandtl-Darcy convection in a vertical porous layer". *International Journal of Heat and Mass Transfer,* **31**, pp. 1529–1534.

[12] Straughan, B., 1988. "A nonlinear analysis of convection in a porous vertical slab". *Geophysical & Astrophysical Fluid Dynamics,* **42**, pp. 269–275.

[13] Rees, D. A. S., 2011. "The effect of local thermal nonequilibrium on the stability of convection in a vertical porous channel". *Transport in Porous Media,* **87**, pp. 459–464.

[14] Scott, N. L., and Straughan, B., 2013. "A nonlinear stability analysis of convection in a porous vertical channel including local thermal nonequilibrium". *Journal of Mathematical Fluid Mechanics,* **15**, pp. 171–178.

[15] Barletta, A., and Alves, L. S. de B., 2014. "On Gill's stability problem for non-Newtonian Darcy's flow". *In-*

ternational Journal of Heat and Mass Transfer, **79**, pp. 759–768.

[16] Barletta, A., 2015. "A proof that convection in a porous vertical slab may be unstable". *Journal of Fluid Mechanics,* **770**, pp. 273–288.

[17] McKibbin, R., 1986. "Thermal convection in a porous layer: effects of anisotropy and surface boundary conditions". *Transport in Porous Media,* **1**, pp. 271–292.

[18] Storesletten, L., 2004. "Effects of anisotropy on convection in horizontal and inclined porous layers". In Emerging Technologies and Techniques in Porous Media, D. B. Ingham, A. Bejan, E. Mamut, and I. Pop, eds., Springer Netherlands, pp. 285–306.

[19] Kvernvold, O., and Tyvand, P. A., 1979. "Nonlinear thermal convection in anisotropic porous media". *Journal of Fluid Mechanics,* **90**, pp. 609–624.

[20] Nilsen, T., and Storesletten, L., 1990. "An analytical study on natural convection in isotropic and anisotropic porous channels". *JOURNAL OF HEAT TRANSFER–TRANSACTIONS OF THE ASME,* **112**, pp. 396–401.

[21] Rees, D., and Postelnicu, A., 2001. "The onset of convection in an inclined anisotropic porous layer". *International Journal of Heat and Mass Transfer,* **44**, pp. 4127–4138.

[22] Straughan, B., 2019. "Anisotropic bidispersive convection". *Proceedings of the Royal Society A,* **475**(2019.0206), pp. 1–18.

[23] Storesletten, L., and Rees, D. A. S., 2019. "Onset of convection in an inclined anisotropic porous layer with internal heat generation". *Fluids,* **4**(75), pp. 1–18.

[24] Naveen, S. B., Shankar, B. M., and Shivakumara, I. S., 2021. "Stability of natural convection in a vertical anisotropic porous channel with oblique principal axes under thermal nonequilibrium conditions". In Advances in Fluid Dynamics, B. Rushi Kumar, R. Sivaraj, and J. Prakash, eds., Springer, pp. 641–652.